Author Manuscript
Author Manuscript
Author Manuscript
Author Manuscript

HHS Public Access
Author manuscript
Radiother Oncol. Author manuscript; available in PMC 2022 June 01.

Published in final edited form as:
Radiother Oncol. 2021 June ; 159: 39–47. doi:10.1016/j.radonc.2021.03.008.

Anatomic changes in head and neck intensity-modulated proton therapy: comparison between robust optimization and online adaptation

Arthur Lalonde[a], **Mislav Bobić**[a,b], **Brian Winey**[a], **Joost Verburg**[a], **Gregory C. Sharp**[a], **Harald Paganetti**[a]

[a] Department of Radiation Oncology, Massachusetts General Hospital & Harvard Medical School, Boston, Massachusetts, USA [b] ETH Zürich, Zürich, Switzerland

Abstract

Background/purpose: Setup variations and anatomical changes can severely affect the quality of head and neck intensity-modulated proton therapy (IMPT) treatments. The impact of these changes can be alleviated by increasing the plan's robustness *a priori*, or by adapting the plan online. This work compares these approaches in the context of head and neck IMPT.

Materials/methods: A representative cohort of 10 head and neck squamous cell carcinoma (HNSCC) patients with daily cone-beam computed tomography (CBCT) was evaluated. For each patient, three IMPT plans were created: 1- a classical robust optimization (cRO) plan optimized on the planning CT, 2- an anatomical robust optimization (aRO) plan additionally including the two first daily CBCTs and 3- a plan optimized without robustness constraints, but online-adapted (OA) daily, using a constrained spot intensity re-optimization technique only.

Results: The cumulative dose following OA fulfilled the clinical objective of both the high-risk and low-risk clinical target volumes (CTV) coverage in all 10 patients, compared to 8 for aRO and 4 for cRO. aRO did not significantly increase the dose to most organs at risk compared to cRO, although the integral dose was higher. OA significantly reduced the integral dose to healthy tissues compared to both robust methods, while providing equivalent or superior target coverage.

Conclusion: Using a simple spot intensity re-optimization, daily OA can achieve superior target coverage and lower dose to organs at risk than robust optimization methods.

Keywords

Intensity-modulated proton therapy; Online-adaptive proton therapy; Robust treatment planning; Anatomical changes; Head and Neck cancer

Corresponding author: Arthur Lalonde, PhD, Massachusetts General Hospital and Harvard Medical School, 55 Fruit Street, 02114 Massachusetts, USA. alalonde@mgh.harvard.edu.

Conflict of interest: The authors have no conflict of interest to declare.

Publisher's Disclaimer: This is a PDF file of an unedited manuscript that has been accepted for publication. As a service to our customers we are providing this early version of the manuscript. The manuscript will undergo copyediting, typesetting, and review of the resulting proof before it is published in its final form. Please note that during the production process errors may be discovered which could affect the content, and all legal disclaimers that apply to the journal pertain.

Author Manuscript Author Manuscript Author Manuscript Author Manuscript

Introduction

Radiation-induced toxicities are an important concern for patients undergoing radiation therapy of the head and neck region, as common long-term effects, such as xerostomia and dysphagia, can have a significant impact on their quality of life [1]. For this reason, a strong interest in using intensity-modulated proton therapy (IMPT) for the treatment of head and neck squamous cell carcinomas (HNSCC) has emerged over the past few years [2]. Compared to photon radiotherapy, IMPT has the potential to reduce the dose to organs at risk (OAR), while providing equivalent to superior target coverage [3–7]. However, the sharp dose fall-off created by proton beams makes IMPT more sensitive than photon radiation therapy against setup and anatomical variations, which are common amongst head and neck patients. This can lead to a severe degradation of the treatment plan, requiring time and resource consuming replanning [8,9].

In order to maintain the benefits of IMPT amid anatomical changes and setup variations, several robust optimization approaches have been proposed [10]. In addition to the nominal scenario, these methods explicitly account for different uncertainty sources during the optimization process, substantially reducing the sensitivity of the final plan toward these uncertainties. Classical robust optimization (cRO), which typically considers setup and range uncertainties, has been investigated for HNSCC [11–14]. More recently, anatomical robust optimization (aRO), which additionally include non-rigid anatomical variations during the optimization process, has been shown to reduce the need of replanning in HNSCC patients [15–18]. However, since several uncertainty scenarios have to be considered simultaneously, robustness is generally achieved at the cost of an increased integral dose to healthy tissues [19, 20].

A different approach that can be used to uphold the dosimetric benefits of IMPT over the course of a fractionated treatment is to adapt the plan online, at each fraction [18, 21–23]. Compared to offline replanning, online adaptation (OA) has the advantage of not delaying nor interrupting the treatment schedule and allows the adapted plan to reflect the exact patient position and anatomy. Different types of OA might be performed in the future, ranging from full replanning [21, 24] to limited plan restoration techniques [22, 23]. For prostate patients, a recent simulation study has shown that a simple daily spot-intensity re-optimization technique could achieve superior target coverage and lower dose to OAR than robust optimization, and similar outcomes as full re-optimization [25]. However, such an evaluation is yet to be done in head and neck patients.

The aim of this work was to evaluate the benefits of online adaptation compared to robust optimization for the treatment of HNSCC with IMPT, in the presence of realistic setup variations and anatomical changes. For this purpose, a cohort of ten HNSCC patients with daily cone-beam computed tomography (CBCT) was considered. For each patient, two plans were robustly optimized with cRO and aRO respectively, while the other was optimized without robustness constraints, but adapted daily using a constrained spot-intensity re-optimization technique. Dose tracking using deformable image registration of the CBCT images to the planning CT was performed in order to compare the cumulative dose distributions associated with each approach.

Author Manuscript Author Manuscript Author Manuscript Author Manuscript

Methods and Materials

Patient data

Ten HNSCC patients originally treated with volumetric-modulated arc therapy (VMAT) at the Massachusetts General Hospital between July and December 2019 were considered in this retrospective study, as CBCT was not available for our proton patients. For each patient, a planning CT was acquired on a wide bore GE scanner (General Electric Medical Systems, Milwaukee, WI). Each patient dataset additionally included a series of daily CBCTs, obtained on an Elekta XVI system (Elekta AB, Stockholm, Sweden) using a 100 kVp tube voltage and a 220 degree acquisition. The number of daily CBCTs available for each patient ranged between 31 and 35 with a median of 33 CBCT volumes.

Contours delineation was performed by an experienced radiation oncologist on the planning CT. Two clinical target volumes (CTV) were defined: a high-risk CTV, which included the primary tumour and adjacent high-risk lymph nodes, as well as a low-risk CTV, encompassing bilateral lymph nodes considered at risk to harbor subclinical disease. Parotid glands, spinal cord, constrictor muscles, esophagus, oral cavity, larynx and brainstem were additionally contoured and treated as OARs. Relevant clinical details of our patient cohort including tumor location, disease staging and weight change during treatment are listed in Supplementary File I.

As patients considered in this study were originally treated with photon radiotherapy, most of them only had a single contrast-enhanced CT available for treatment planning purposes. The presence of contrast agent in single-energy CT images is known to affect dose calculation in proton therapy [26, 27], therefore we mitigated that effect by delineating regions of high contrast uptake in the treatment planning system and set their density to the one of soft tissue (1.05 g/cm^3).

Treatment planning

For each patient, three treatment plans were created in RayStation (v8.99, Raysearch Laboratories, Stockholm, Sweden): 1) a classical robust optimization (cRO) using a 3 mm setup uncertainty, 2) an anatomical robust optimization (aRO) using the same criteria as cRO, but optimized simultaneously on the planning CT and the two first fractions' CBCTs to include realistic variability in patient positioning and 3) a plan optimized without robustness constraints, but online-adapted (OA) on each CBCT using a constrained spot intensity re-optimization technique only. In practice, aRO would include several planning CTs obtained before treatment to reflect potential non-rigid patient anatomy variations [19], but those were not available for our patients. Similarly as Cubillos-Mesías *et al.* [15, 17], we instead used CBCT data from the two first fractions of each patient in order to introduce realistic non-rigid variations without substantial treatment-induced anatomical changes.

The minimax approach [28] was used to create both robust plans, enforcing robustness to the dose constraints of both CTVs, the spinal cord, the brainstem and the parotid glands. In order to isolate the impact of anatomical changes and setup variations on target coverage, it was assumed that all uncertainties not directly addressed by the daily CBCT data, i.e. all

Author Manuscript Author Manuscript Author Manuscript Author Manuscript

except for setup and patient anatomy, were considered in the original volumes definition, similarly as in Botas *et al.* [23].

All plans were created using a simultaneous integrated boost (SIB) technique, with a prescribed mean dose of 57 Gy and 70 Gy to the low-risk and high-risk CTV respectively, in the same number of fractions as available daily CBCTs for each patient. An intermediate region of 10 mm was created between the low- and high-risk CTV to foster a steep dose gradient between the two regions. The following constraints were applied to both target volumes: $D_{98\%} \geq 95\%$ and $D_{2\%} \leq 107\%$ of the prescription dose, where $D_{98\%}$ and $D_{2\%}$ are the minimum doses to 98% and 2% of the target volume respectively. For the OARs, mean or maximum dose (D_{mean} and D_{max}) constraints were used as follows: $D_{max} < 45$ Gy in the spinal cord, $D_{mean} < 26$ Gy to both parotids individually, $D_{mean} < 42$ Gy to the constrictor muscles, $D_{max} < 54$ Gy to the brainstem, $D_{mean} < 40$ Gy to the larynx. Plans were optimized with multi-criteria optimization considering all OARs listed above, in addition to oral cavity and esophagus, for which dose was kept as low as reasonably achievable.

All plans were created using the *IBA Dedicated Nozzle* beam model (spot size in air at 150 MeV of 3.73 mm), with beam angles of 60°, 180° and 300°, a 40 mm range shifter, a 30 mm minimum air gap and spot spacing factor of 1. Dose calculation was performed with the Monte Carlo algorithm of RayStation in a $2.0 \times 2.0 \times 2.0$ mm^3 dose grid and a relative biological effectiveness (RBE) of 1.1.

Online adaptation

Online adaptation was performed as outlined in Figure 1 using an in-house developed workflow. First, the daily CBCT images were corrected for scatter artifacts using a fast deep-learning based method validated for proton therapy dose calculation [29]. Then, contours from the planning CT were propagated to the scatter-corrected daily CBCT using the graphics processing unit (GPU) parallelized B-spline deformable image registration (DIR) algorithm Plastimatch [30]. The accuracy of the propagated contours was visually verified for each CBCT. The GPU accelerated Monte Carlo dose calculation algorithm gPMC [31] was then executed to derive the dose associated with each beamlet of the IMPT treatment plan on the corrected CBCT images, using the same beam model as in RayStation. From there, plan restoration was performed by only re-optimizing the intensity of a subset of spots with Opt4D [32], an in-house developed optimization tool. The same objectives and constraints as for the initial treatment plan were used for adaptation. Contrary to the online adaptation methods of Botas *et al.* [23] and Jagt *et al.* [25], the energy and position of the spots were not modified, in order to constrain the level of deviation from the original treatment plan allowed and to reduce the risk of obtaining undeliverable treatment plans. In cases with severe anatomical changes, additional energy layers would be required to achieve target coverage. Our methodology specifically does not consider such cases as we aim at providing deviations from the original plan that are limited to beamlet weight changes to potentially avoid elaborate quality assurance (QA) processes needed for an entirely new plan which could make OA impractical or even infeasible. Severe changes would result in the need for replanning with a threshold defined by whether our algorithm is able to find an

Author Manuscript Author Manuscript Author Manuscript Author Manuscript

acceptable adapted plan. This was however not the case for any of our cohort patients, despite the important weight change some experienced.

Similarly as in Botas *et al.* [23], the spots selected for intensity re-optimization were defined as the smallest set of beamlets carrying at least 33% of the total spots' intensity, with the constraint that the number of spots selected represented at least 10% of the total number of beamlets. No constraints were applied to the proportion of spots selected for each field, although the re-optimized spots were generally evenly distributed within all three beams. The average number of spots selected for weight tuning within our patient cohort was 896, while the average number of spots per treatment plan was 7632.

Dose accumulation and data analysis

For each treatment plan, dose distributions were calculated on the corrected daily CBCTs and deformed to the planning CT for dose accumulation. Dose calculation on the daily CBCTs was performed using RayStation (with Monte Carlo) for cRO and aRO, while gPMC was used for OA. This way, any potential discrepancies between gPMC and RayStation would be intrinsically addressed by OA without affecting the robust methods. Dose-volume metrics were evaluated on the cumulative dose distributions in order to establish the performance of each method. The statistical significance of the differences between the dose metrics of each approach was evaluated using Wilcoxon signed-rank tests, considering a p-value <.05 as statistically significant.

Results

Nominal and cumulative dose statistics are presented for each method in Table 1. All plans met the clinical goals in the nominal scenario, both in terms of target coverage and OAR constrains. In the cumulative scenario, target coverage ($D_{98\%}$) of the low-risk CTV was significantly lower for cRO and aRO compared to OA (p=.002 and p=.014 respectively), with median values of 95.06%, 96.54% and 97.97% respectively. A similar trend was observed in the high-risk CTV, with median values of 96.58%, 97.47%, 98.07% for cRO, aRO and OA respectively. Once again, difference between cRO and aRO with respect to OA were significant (p=.002 and p=.004). Differences in the cumulative $D_{98\%}$ values between cRO and aRO were also significant for both CTVs (p=.002 and p=.010 for low-risk and high-risk CTVs respectively). The overdosage of the high-risk CTV, reflected in $D_{2\%}$, was not significantly different between the three methods.

Cumulative target coverages are presented for each patient individually in Figure 2. Of all three methods, only OA was able to achieve a cumulative $D_{98\%}$ over 95% for both CTVs simultaneously in all patients, although aRO met this criterium 8 times out of 10. With cRO, target underdosage was more common in the low-risk CTV (5 patients out of 10) than in the high-risk one (2 patients out of 10). The distributions of cumulative dose statistics to OARs are presented in Figure 3. Comparing the two robust methods together, one can see that the increased robustness of aRO over cRO is not achieved at the cost of a significantly higher dose to most OARs, although the integral dose was increased.

Author Manuscript Author Manuscript Author Manuscript Author Manuscript

The evolution of target coverage over the course of treatment is presented for five representative patients in Figure 4. Some of them, like patient 2 and 3, exhibited a continuous degradation of the target coverage for both robust optimization methods, especially perceptible in the low-risk CTV. Both patients experienced a progressive weight loss during treatment. Some other patients, like patients 5 and 10, display irregular fluctuations of the coverage in the high-risk CTV, which were more likely associated with an inconsistent positioning of the target from fraction to fraction. Dose distributions associated with three of these patients are shown in Figure 5. For patient 2, where the weight loss was less severe than for patient 3, cold spots are visible in the low-risk CTV of cRO, but not in aRO nor OA. However, one can see that the 35 Gy isodose line is more conformal to the target volume in OA than in aRO, which highlights the reduced integral dose associated with the former approach. For patient 3, who experienced more significant weight loss, both robust approaches yielded cold spots in the low-risk CTV, as neither of them could anticipate such drastic changes in the patient's anatomy. Finally, in patient 5, variations in the positioning of the high-risk CTV during treatment induced a cold spot for cRO, but not in aRO. This patient was treated for a base of tongue tumor, for which consistent positioning is particularly challenging. In this case, aRO was able to achieve satisfying coverage, as representative variable positions of the tongue were covered by the additional scenarios introduced to optimize the plan. Nonetheless, OA was able to achieve target coverage in both patients 3 and 5, which demonstrates the robustness of the approach toward the type of variations affecting the treatments.

Discussion

In this study, we compared three strategies to maintain the dosimetric benefits of IMPT for HNSCC treatments in the presence of setup variations and anatomic changes. Our results demonstrated the benefits of online adaptation to restore initial treatment plan quality of head and neck IMPT plans using a simple spot intensity re-optimization technique. With this strategy, OA was able to meet the clinical goals for both CTVs simultaneously in all 10 patients, compared to 8/10 and 4/10 for anatomical and classical robust optimization respectively. This suggests that the clinical implementation of a simple OA workflow could be beneficial for the subset of patients where robust treatment plans fail to ensure target coverage and for whom disruptive replanning would otherwise be needed. This finding is similar to what was reported in prostate patients by Jagt *et al.* [25] and for sinonasal tumors by van de Water *et al.* [18], where a daily online dose restoration method provided superior target coverage and better OAR sparing than robust optimization approaches.

Our study also supports the superiority of anatomical robust optimization, also known as multiple-CT optimization [16, 33], over classical robust optimization for the treatment of HNSCC, as reported by Cubillos-Mesías *et al.* [15, 17]. Similar findings were also made by Wang *et al.* [33] and Li *et al.* [34] for lung treatments and by van de Water *et al.* [18] for sinonasal tumours. Based on daily CBCTs instead to weekly CTs, our investigation additionally highlighted the daily fluctuations of patients' setup and anatomy. In that regard, our results indicated that the benefits of aRO over cRO were especially important in patients where the reproducibility of target positioning is more challenging, such as for base of tongue tumors. Although increasing setup robustness for these cases could be considered, it

Author Manuscript Author Manuscript Author Manuscript Author Manuscript

is interesting to see that OA has the potential to compensate the limitations of immobilization hardware.

Our results also indicated that the benefits of aRO over cRO were not acquired at the cost of a significantly higher dose to OARs, but at a significant increase of the integral dose. This was also observed by Cubillos-Mesías *et al.* [15], which tends to demonstrate that using aRO over cRO is appropriate in order to increase target coverage without compromising critical structures. However, our data also indicates that OA has the potential to significantly reduce the dose to most OARs as well as the integral dose to healthy tissues, and an equivalent to superior target coverage compared to robust methods. Eliminating all additional dose needed to account for anatomical changes and setup variations resulted in a reduction in the dose to healthy tissues of 18.70% for OA compared to aRO. The low dose volume shrinkage associated with OA seemed to be particularly beneficial to OARs situated further from the target volume, such as the spinal cord, where the median D_{1cc} was reduced by more than 50% with OA over cRO and aRO. For OARs closer to the target, like the parotids, and especially the ipsilateral one, smaller gains were observed, and those were not statistically significant.

A critical aspect of online adaptation is the time requirement. In our patient cohort, the total time for treatment adaption ranged between 8 and 22 minutes, with a median time of 12 minutes. The time was approximately distributed as follows: 5 seconds for CBCT scatter-correction, 2 minutes for contour propagation, 4 minutes for dose calculation and 6 minutes for spot intensity re-optimization. While this might be clinically acceptable, several strategies could be investigated to improve the efficiency of our workflow. For instance, the use of a multi-GPU system should substantially reduce the time required for deformable image registration as well as Monte Carlo dose calculation [23]. Since our workflow is mostly automated, some user-related tasks could also be done in parallel, in order to limit the total time required for plan adaptation. For example, visual inspection of the propagated contours, which is not included in the total time reported above, can be performed while the dose-influence matrix of the beamlets are being calculated. Another challenge facing the clinical implementation of online adaptation of IMPT treatments that was not tackled by this work is the QA of the adapted plan. While QA would arguably be simplified using our weight tuning approach over full re-optimization or complete replanning, log file-based analysis could be considered [35], as well as *in vivo* range verification using prompt gamma detection [36, 37]. Finally, different adaptation frequencies could be considered if the time and resource requirements of OA are found to be impractical for daily use [38].

A limitation of this work is the use of CBCT images for dose calculation, which was necessary in order to accurately reflect the effect of daily setup variations and anatomical changes. Dose calculation based on CBCT data is known to be challenging [39, 40], and this had the potential to introduce an additional level of plan degradation for the cRO case, which was optimized on CT data only. To mitigate this effect, all CBCT images used in this study were corrected with a projection-based method that was previously validated in phantom and patient images, achieving millimetric agreement in range prediction between CT and scatter-corrected CBCT images, as well as 3%/3mm gamma pass-rate above 98% in HNSCC plans [29]. Considering the fact that stopping power accuracy has a limited impact on target

Author Manuscript Author Manuscript Author Manuscript Author Manuscript

coverage compared to anatomical changes in head and neck patients [17], we believe that scatter-corrected CBCTs were a reasonable surrogate to daily CT data for the purpose of this work.

Another limitation worth mentioning is the assumption that all uncertainty sources other than setup and anatomical variations affected equally the three methods and could therefore have been considered at the target definition stage. This includes range uncertainty, which we did not explicitly incorporated in the robust optimization and online adaptation. By including range uncertainty in the robust optimization and then relying on the daily CBCTs to recalculate the delivered doses, we could have overestimated target coverage, as robustness against range uncertainties could artificially compensate anatomical changes in the beam's direction. We instead treated range uncertainties as if they were included in the target volumes' definition, which was suitable for the purpose of this work since the estimated range accuracy was similar for all methods and because beams arrangement was not changed for adaptation. While these conditions are representative of most foreseeable clinical scenarios, there are some situations where it might not be the case, for instance if substantially different imaging modalities were used for treatment planning and adaptation (e.g. dual-energy CT for planning [41, 42] and MRI for adaptation [43, 44]), if fundamentally different dose calculation algorithms were used for planning and adaptation [45], or if *in vivo* range verification was available for OA [36, 37]. In such cases, range uncertainties would be different for online adaptation and robust treatment planning, and this could have an impact on the relative performance of each method reported in this work. Studying the effects of variable levels of uncertainty for sources other than setup and anatomical changes on the benefits of OA over robust methods was out of the scope of this study, but warrants further investigations.

Finally, it should be noted that the same deformation fields were used to propagate the contours for OA and to accumulate the dose for all methods. Our results therefore reflect the best-case scenario of OA, where DIR accuracy for contour propagation is neglected. In a clinical scenario, the level of scrutiny applied to the daily contours would have to be balanced between the desired accuracy and the time constraints, something we did not tackle in this work. It is also important to stress out that our work was based on CBCT data from VMAT patients, which might differ from IMPT patients in terms of setup reproducibility and response to treatment. The positioning protocols at our institutions are however very similar between IMPT and VMAT, except that we typically use slightly different immobilization masks for each modality.

Globally, our study suggests that online adaptation of IMPT plans based on a simple spot-intensity re-optimization has the potential to increase treatment quality for HNSCC compared to state-of-the-art robust optimization methods. The main benefits of this approach over robust methods were an improved target coverage, reduced integral dose and the fact that it performed similarly well in cases exhibiting random positioning fluctuations as those with more drastic anatomical changes, this without relying on disruptive re-planning.

Author Manuscript Author Manuscript Author Manuscript Author Manuscript

Supplementary Material

Refer to Web version on PubMed Central for supplementary material.

Acknowledgments:

The authors would like to thank the RaySearch Laboratories AB (Stockholm, Sweden) for providing a non-clinical software license for the RayStation treatment planning system as well as the NVIDIA Corporation for the donation of a Titan Xp GPU used for this research.

Funding statement: This work was funded by the National Cancer Institute (NCI R01CA229178, Fast Individualized Delivery Adaptation in Proton Therapy). Arthur Lalonde was supported by fellowships from the Natural Sciences and Engineering Research Council of Canada (NSERC, PDF-532784 – 2019) and the Fonds de recherche du Quebec - Nature et Technologies (FRQNT, 267388).

REFERENCES

1. Kjaer T, Dalton SO, Andersen E, Karlsen R, Nielsen AL, Hansen MK, ... & Johansen C (2016). A controlled study of use of patient-reported outcomes to improve assessment of late effects after treatment for head-and-neck cancer. Radiotherapy and Oncology, 119(2), 221–228. [PubMed: 27178143]
2. Moreno AC, Frank SJ, Garden AS, Rosenthal DI, Fuller CD, Gunn GB, ... & Phan J (2019). Intensity modulated proton therapy (IMPT)–The future of IMRT for head and neck cancer. Oral oncology, 88, 66–74. [PubMed: 30616799]
3. van der Laan HP, van de Water TA, van Herpt HE, Christianen ME, Bijl HP, Korevaar EW, ... & Langendijk JA (2013). The potential of intensity-modulated proton radiotherapy to reduce swallowing dysfunction in the treatment of head and neck cancer: A planning comparative study. Acta oncologica, 52(3), 561–569. [PubMed: 22708528]
4. Góra J, Kuess P, Stock M, Andrzejewski P, Knäusl B, Paskeviciute B, ... & Georg D (2015). ART for head and neck patients: On the difference between VMAT and IMPT. Acta Oncologica, 54(8), 1166–1174. [PubMed: 25850583]
5. Blanchard P, Garden AS, Gunn GB, Rosenthal DI, Morrison WH, Hernandez M, ... & Mohamed AS (2016). Intensity-modulated proton beam therapy (IMPT) versus intensity-modulated photon therapy (IMRT) for patients with oropharynx cancer–a case matched analysis. Radiotherapy and Oncology, 120(1), 48–55. [PubMed: 27342249]
6. Barten DL, Tol JP, Dahele M, Slotman BJ, & Verbakel WF (2015). Comparison of organ-at-risk sparing and plan robustness for spot-scanning proton therapy and volumetric modulated arc photon therapy in head-and-neck cancer. Medical physics, 42(11), 6589–6598. [PubMed: 26520750]
7. Jakobi Annika, et al. “Identification of patient benefit from proton therapy for advanced head and neck cancer patients based on individual and subgroup normal tissue complication probability analysis.” International Journal of Radiation Oncology* Biology* Physics 92.5 (2015): 1165–1174.
8. Stützer K, Jakobi A, Bandurska-Luque A, Barczyk S, Arnsmeyer C, Löck S, & Richter C (2017). Potential proton and photon dose degradation in advanced head and neck cancer patients by intratherapy changes. Journal of applied clinical medical physics, 18(6), 104–113.
9. Müller BS, Duma MN, Kampfer S, Nill S, Oelfke U, Geinitz H, & Wilkens JJ (2015). Impact of interfractional changes in head and neck cancer patients on the delivered dose in intensity modulated radiotherapy with protons and photons. Physica Medica, 31(3), 266–272. [PubMed: 25724350]
10. Unkelbach J, Alber M, Bangert M, Bokrantz R, Chan TC, Deasy JO, ... & Mahmoudzadeh H (2018). Robust radiotherapy planning. Physics in Medicine & Biology, 63(22), 22TR02.
11. Liu W, Frank SJ, Li X, Li Y, Park PC, Dong L, ... & Mohan R (2013). Effectiveness of robust optimization in intensity-modulated proton therapy planning for head and neck cancers. Medical physics, 40(5), 051711. [PubMed: 23635259]
12. Cubillos-Mesías M, Baumann M, Troost EG, Lohaus F, Löck S, Richter C, & Stützer K (2017). Impact of robust treatment planning on single-and multi-field optimized plans for proton beam

Author Manuscript Author Manuscript Author Manuscript Author Manuscript

therapy of unilateral head and neck target volumes. Radiation Oncology, 12(1), 190. [PubMed: 29183377]

13. van Dijk LV, Steenbakkers RJ, ten Haken B, van der Laan HP, van ‘t Veld AA, Langendijk JA, & Korevaar EW (2016). Robust intensity modulated proton therapy (IMPT) increases estimated clinical benefit in head and neck cancer patients. PLoS One, 11(3), e0152477. [PubMed: 27030987]
14. Hague C, Aznar M, Dong L, Fotouhi-Ghiam A, Lee LW, Li T, ... & O’Reilly S (2020). Inter-fraction robustness of intensity-modulated proton therapy in the post-operative treatment of oropharyngeal and oral cavity squamous cell carcinomas. The British Journal of Radiology, 93(1107), 20190638. [PubMed: 31845816]
15. Cubillos-Mesías M, Troost EG, Lohaus F, Agolli L, Rehm M, Richter C, & Stützer K (2019). Including anatomical variations in robust optimization for head and neck proton therapy can reduce the need of adaptation. Radiotherapy and Oncology, 131, 127–134. [PubMed: 30773179]
16. Yang Z, Zhang X, Wang X, Zhu XR, Gunn B, Frank SJ, ... & Liao L (2020). Multiple-CT optimization: An adaptive optimization method to account for anatomical changes in intensity-modulated proton therapy for head and neck cancers. Radiotherapy and Oncology, 142, 124–132. [PubMed: 31564553]
17. Cubillos-Mesías M, Troost EG, Lohaus F, Agolli L, Rehm M, Richter C, & Stützer K (2020). Quantification of plan robustness against different uncertainty sources for classical and anatomical robust optimized treatment plans in head and neck cancer proton therapy. The British Journal of Radiology, 93(1107), 20190573. [PubMed: 31778315]
18. van de Water S, Albertini F, Weber DC, Heijmen BJ, Hoogeman MS, & Lomax AJ (2018). Anatomical robust optimization to account for nasal cavity filling variation during intensity-modulated proton therapy: a comparison with conventional and adaptive planning strategies. Physics in Medicine & Biology, 63(2), 025020. [PubMed: 29160775]
19. van de Water S, van Dam I, Schaart DR, Al-Mamgani A, Heijmen BJ, & Hoogeman MS (2016). The price of robustness; impact of worst-case optimization on organ-at-risk dose and complication probability in intensity-modulated proton therapy for oropharyngeal cancer patients. Radiotherapy and Oncology, 120(1), 56–62. [PubMed: 27178142]
20. Chen W, Unkelbach J, Trofimov A, Madden T, Kooy H, Bortfeld T, & Craft D (2012). Including robustness in multi-criteria optimization for intensity-modulated proton therapy. Physics in Medicine & Biology, 57(3), 591. [PubMed: 22222720]
21. Nenoff L, Matter M, Hedlund Lindmar J, Weber DC, Lomax AJ, & Albertini F (2019). Daily adaptive proton therapy–the key to innovative planning approaches for paranasal cancer treatments. Acta oncologica, 58(10), 1423–1428. [PubMed: 31364904]
22. Bernatowicz K, Geets X, Barragan A, Janssens G, Souris K, & Sterpin E (2018). Feasibility of online IMPT adaptation using fast, automatic and robust dose restoration. Physics in Medicine & Biology, 63(8), 085018. [PubMed: 29595145]
23. Botas P, Kim J, Winey B, & Paganetti H (2018). Online adaption approaches for intensity modulated proton therapy for head and neck patients based on cone beam CTs and Monte Carlo simulations. Physics in Medicine & Biology, 64(1), 015004. [PubMed: 30524097]
24. Jagt TZ, Breedveld S, Van Haveren R, Nout RA, Astreinidou E, Heijmen BJ, & Hoogeman MS (2019). Plan-library supported automated replanning for online-adaptive intensity-modulated proton therapy of cervical cancer. Acta Oncologica, 58(10), 1440–1445. [PubMed: 31271076]
25. Jagt TZ, Breedveld S, van Haveren R, Heijmen BJ, & Hoogeman MS (2020). Online-adaptive versus robust IMPT for prostate cancer: how much can we gain?. Radiotherapy and Oncology.
26. Lalonde A, Xie Y, Burgdorf B, O’Reilly S, Ingram WS, Yin L, ... & Teo BKK (2019). Influence of intravenous contrast agent on dose calculation in proton therapy using dual energy CT. Physics in Medicine & Biology, 64(12), 125024. [PubMed: 31044743]
27. Wertz H, & Jäkel O (2004). Influence of iodine contrast agent on the range of ion beams for radiotherapy. Medical physics, 31(4), 767–773. [PubMed: 15124994]
28. Fredriksson A, Forsgren A, & Hårdemark B (2011). Minimax optimization for handling range and setup uncertainties in proton therapy. Medical physics, 38(3), 1672–1684. [PubMed: 21520880]

Author Manuscript Author Manuscript Author Manuscript Author Manuscript

29. Lalonde A, Winey B, Verburg J, Paganetti H, & Sharp GC (2020). Evaluation of CBCT scatter correction using deep convolutional neural networks for head and neck adaptive proton therapy. Physics in Medicine & Biology, 65(24), 245022.
30. Sharp GC, Li R, Wolfgang J, Chen G, Peroni M, Spadea MF, ... & Kandasamy N (2010, June). Plastimatch: an open source software suite for radiotherapy image processing. In Proceedings of the XVI'th International Conference on the use of Computers in Radiotherapy (ICCR), Amsterdam, Netherlands.
31. Qin N, Botas P, Giantsoudi D, Schuemann J, Tian Z, Jiang SB, ... & Jia X (2016). Recent developments and comprehensive evaluations of a GPU-based Monte Carlo package for proton therapy. Physics in Medicine & Biology, 61(20), 7347. [PubMed: 27694712]
32. Trofimov A, Rietzel E, Lu HM, Martin B, Jiang S, Chen GT, & Bortfeld T (2005). Temporo-spatial IMRT optimization: concepts, implementation and initial results. Physics in Medicine & Biology, 50(12), 2779. [PubMed: 15930602]
33. Wang Xianliang, et al. "Multiple-CT optimization of intensity-modulated proton therapy–Is it possible to eliminate adaptive planning?." Radiotherapy and Oncology 128.1 (2018): 167–173. [PubMed: 29054378]
34. Li H, Zhang X, Park P, Liu W, Chang J, Liao Z, ... & Gillin M (2015). Robust optimization in intensity-modulated proton therapy to account for anatomy changes in lung cancer patients. Radiotherapy and Oncology, 114(3), 367–372. [PubMed: 25708992]
35. Winterhalter C, Meier G, Oxley D, Weber DC, Lomax AJ, & Safai S (2019). Log file based Monte Carlo calculations for proton pencil beam scanning therapy. Physics in Medicine & Biology, 64(3), 035014. [PubMed: 30540984]
36. Xie Y, Bentefour EH, Janssens G, Smeets J, Vander Stappen F, Hotoiu L, ... & Prieels D (2017). Prompt gamma imaging for in vivo range verification of pencil beam scanning proton therapy. International Journal of Radiation Oncology* Biology* Physics, 99(1), 210–218.
37. Hueso-González F, Rabe M, Ruggieri TA, Bortfeld T, & Verburg JM (2018). A full-scale clinical prototype for proton range verification using prompt gamma-ray spectroscopy. Physics in Medicine & Biology, 63(18), 185019. [PubMed: 30033938]
38. Bobić M, Lalonde A, Sharp GC, Grassberger C, Verburg JM, Winey BA, ... & Paganetti H (2021). Comparison of weekly and daily online adaptation for head and neck intensity-modulated proton therapy. Physics in Medicine & Biology.
39. Landry G, Nijhuis R, Dedes G, Handrack J, Thieke C, Janssens G, ... & Paganelli C (2015). Investigating CT to CBCT image registration for head and neck proton therapy as a tool for daily dose recalculation. Medical physics, 42(3), 1354–1366. [PubMed: 25735290]
40. Park YK, Sharp GC, Phillips J, & Winey BA (2015). Proton dose calculation on scatter-corrected CBCT image: Feasibility study for adaptive proton therapy. Medical physics, 42(8), 4449–4459. [PubMed: 26233175]
41. Bär E, Lalonde A, Royle G, Lu HM, & Bouchard H (2017). The potential of dual-energy CT to reduce proton beam range uncertainties. Medical physics, 44(6), 2332–2344. [PubMed: 28295434]
42. Wohlfahrt P, Möhler C, Richter C, & Greilich S (2018). Evaluation of stopping-power prediction by dual-and single-energy computed tomography in an anthropomorphic ground-truth phantom. International Journal of Radiation Oncology* Biology* Physics, 100(1), 244–253.
43. Moteabbed M, Schuemann J, & Paganetti H (2014). Dosimetric feasibility of real-time MRI-guided proton therapy. Medical physics, 41(11), 111713. [PubMed: 25370627]
44. Oborn BM, Dowdell S, Metcalfe PE, Crozier S, Mohan R, & Keall PJ (2017). Future of medical physics: real-time MRI-guided proton therapy. Medical physics, 44(8), e77–e90. [PubMed: 28547820]
45. Nenoff L, Matter M, Jarhall AG, Winterhalter C, Gorgisyan J, Josipovic M, ... & Albertini F (2020). Daily adaptive proton therapy: Is it appropriate to use analytical dose calculations for plan adaption?. International Journal of Radiation Oncology* Biology* Physics.

Author Manuscript Author Manuscript Author Manuscript Author Manuscript

- An online adaptive strategy was compared to two robust optimization methods in the context of head and neck IMPT
- Daily CBCT images from 10 representative patients were used to evaluate the impact of setup variations and anatomical changes on each approach
- The most performing robust optimization method achieved adequate target coverage in 8/10 patients
- Online adaptation achieved adequate target coverage in all patients
- The dose to most OAR as well as the integral dose were reduced using online adaptation over robust optimization

Author Manuscript Author Manuscript Author Manuscript Author Manuscript

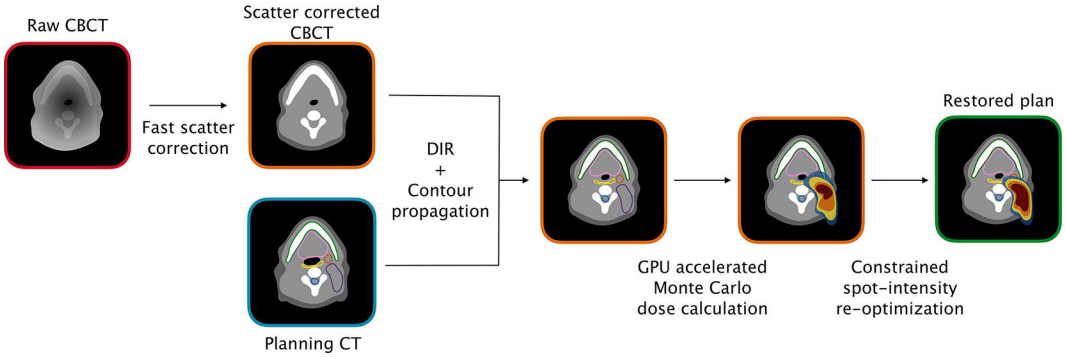

Figure 1 –.

Overview of the online adaptation workflow used in this study. *Abbreviations:* CBCT = cone-beam computed tomography; CT = computed tomography; DIR = deformable image registration; GPU = graphics processing unit.

Author Manuscript Author Manuscript Author Manuscript Author Manuscript

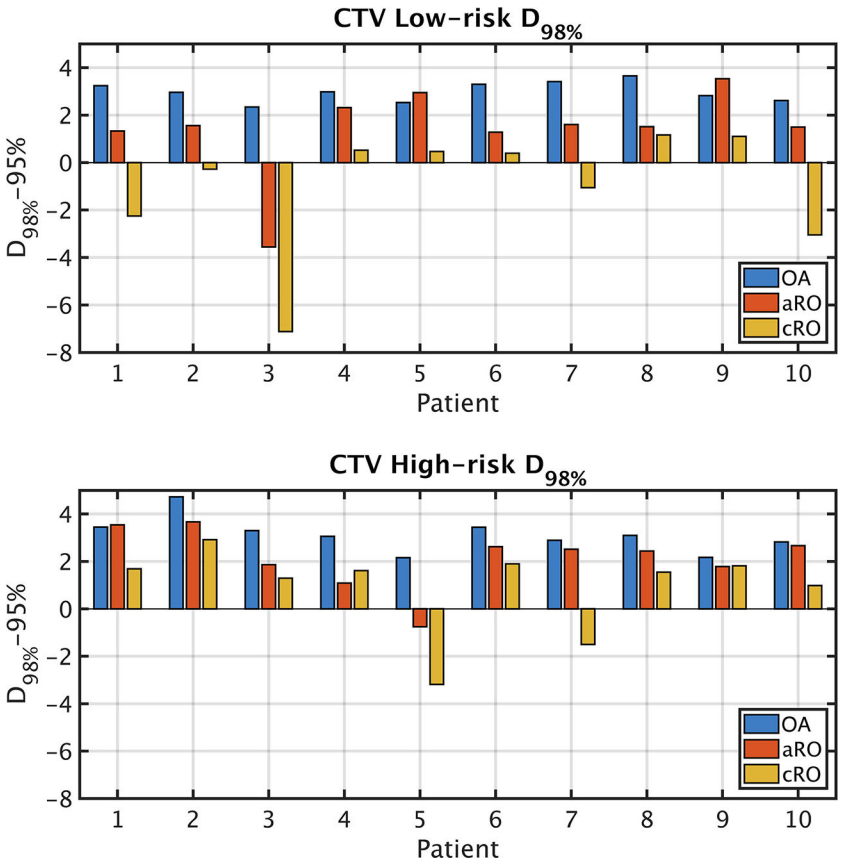

Figure 2 –.

CTV coverage expressed as the difference between the accumulated $D_{98\%}$ in each scenario and 95% of the prescription dose. The differences in $D_{98\%}$ values are statistically significant between all three methods and for both CTVs. *Abbreviations:* CTV = clinical target volume; cRO = classical robust optimization; aRO = anatomical robust optimization; OA = online adaptation.

Author Manuscript Author Manuscript Author Manuscript Author Manuscript

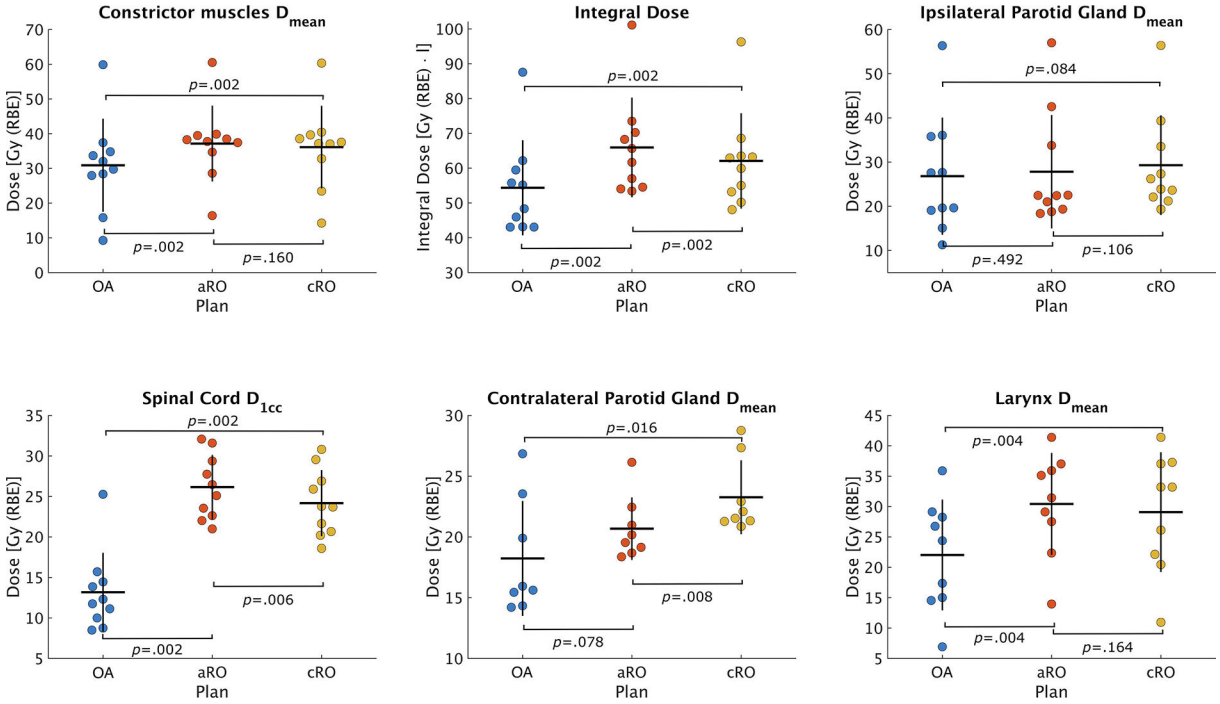

Figure 3 –.

Distribution of dose parameters within the patient cohort derived from the accumulated dose distributions from each scenario. The horizontal line represents the mean value of the distribution, while the vertical line spans over two standard deviations. *Abbreviations:* cRO = classical robust optimization; aRO = anatomical robust optimization; OA = online adaptation.

Author Manuscript Author Manuscript Author Manuscript Author Manuscript

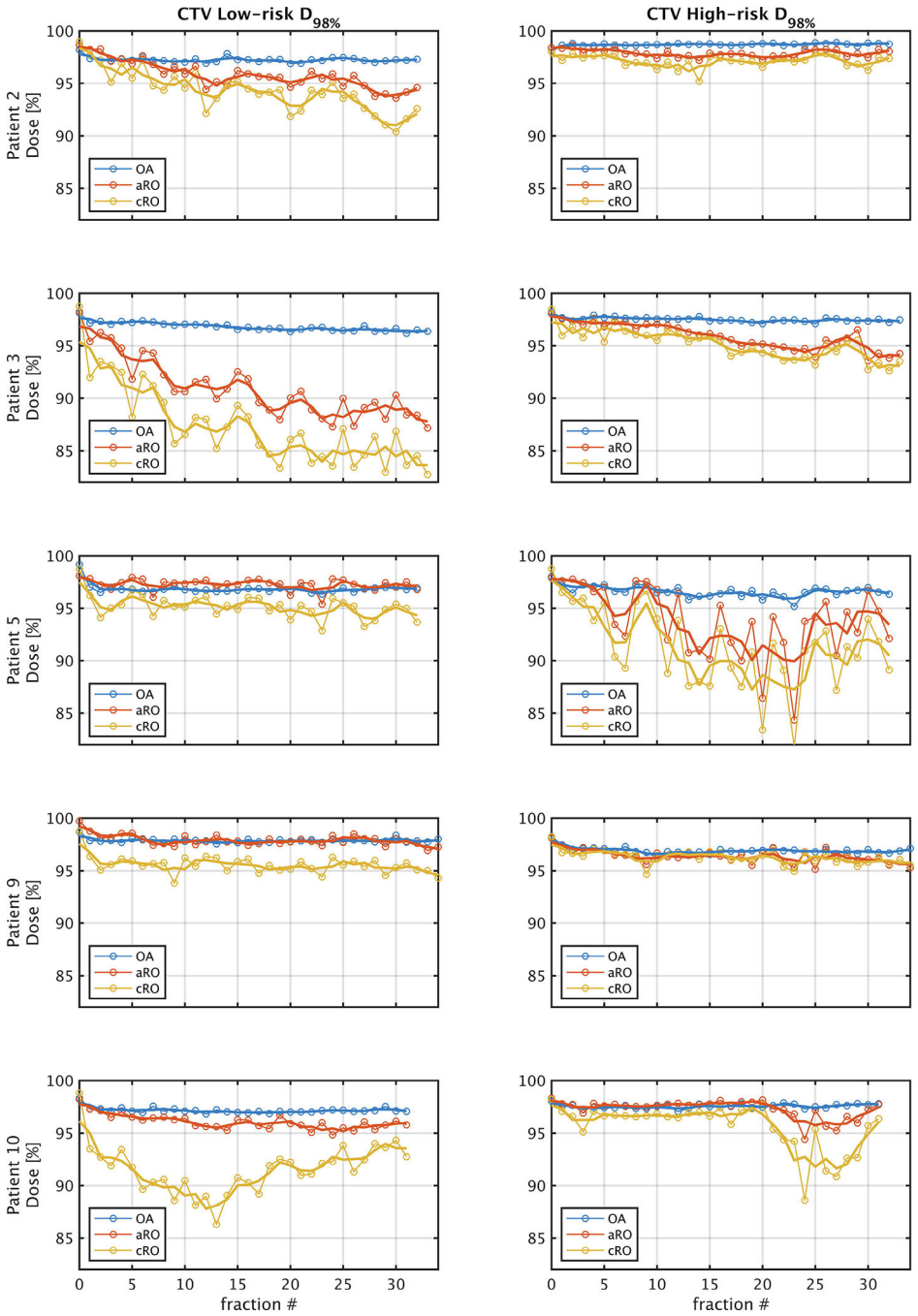

Figure 4 –.

Evolution of $D_{98\%}$ for the Low-risk and High-risk CTVs over the course of treatment for a subset of five representative patients. Fraction 0 represents the nominal dose distribution. The thin lines connect each fraction, while the thick lines show the 3-fraction average value. These values were derived from the CBCT dose distributions deformed to the planning CT. *Abbreviations:* CTV = clinical target volume; cRO = classical robust optimization; aRO = anatomical robust optimization; OA = online adaptation.

Author Manuscript Author Manuscript Author Manuscript Author Manuscript

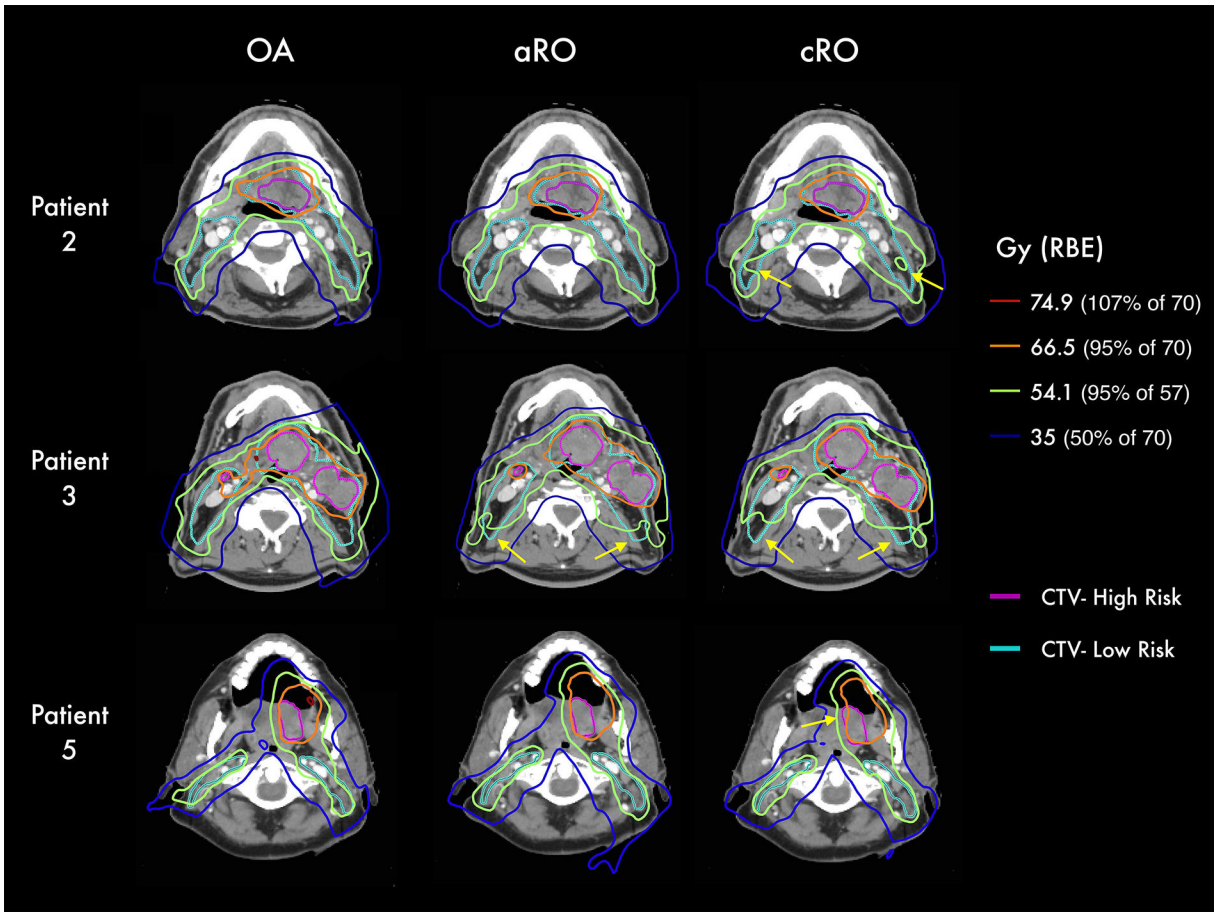

Figure 5 –.

Isodose lines from the accumulated dose distributions of each scenario in three representative patients. Yellow arrows highlight regions of underdosage. *Abbreviations:* CTV = clinical target volume; cRO = classical robust optimization; aRO = anatomical robust optimization; OA = online adaptation.

Author Manuscript Author Manuscript Author Manuscript Author Manuscript

Table 1 -

Dose statistics for the nominal and cumulative dose distributions

ROI	Metric	Dose	Plan median (min-max)		
			cRO	aRO	OA
Low-risk CTV	$D_{98\%}$(%)	Nominal	**98.78** (98.19–99.22)	**98.48** (97.51–99.71)	**98.61** (98.13–99.16)
		Cumulative	**95.06** (87.88–96.17)	**96.54** (91.44–98.53)	**97.97** (97.34–98.65)
High-risk CTV	$D_{98\%}$(%)	Nominal	**98.51** (98.01–98.99)	**98.30** (97.26–98.93)	**98.20** (98.0–98.7)
		Cumulative	**96.58** (91.81–97.92)	**97.47** (94.25–98.66)	**98.07** (97.15–99.73)
	$D_{2\%}$(%)	Nominal	**103.11** (102.43–104.00)	**103.06** (101.74–104.02)	**102.77** (101.91–103.65)
		Cumulative	**102.33** (101.08–103.61)	**102.66** (101.91–104.13)	**102.58** (102.00–103.54)
Spinal Cord	D_{1cc}(Gy)	Nominal	**24.02** (17.78–30.22)	**26.42** (20.04–32.76)	**16.77** (11.83–27.67)
		Cumulative	**23.74** (18.58–30.81)	**25.78** (21.00–32.08)	**12.03** (8.50–25.26)
Ipsilateral Parotid	D_{mean}(Gy)	Nominal	**21.0** (16.33–56.54)	**19.66** (15.72–56.86)	**20.62** (10.75–54.19)
		Cumulative	**25.05** (19.33–56.40)	**22.43** (18.37–57.00)	**23.60** (11.29–56.35)
Contralateral Parotid	D_{mean}(Gy)	Nominal	**19.85** (17.08–21.74)	**18.74** (15.64–20.30)	**15.54** (11.70–21.42)
		Cumulative	**21.43** (18.41–28.76)	**19.85** (18.68–26.14)	**15.78** (14.21–26.85)
Larynx	D_{mean}(Gy)	Nominal	**30.69** (16.73–38.56)	**31.65** (14.76–38.74)	**25.73** (11.75–34.49)
		Cumulative	**33.20** (10.95–41.39)	**31.44** (13.96–41.39)	**24.37** (6.92–35.89)
Constrictor muscles	D_{mean}(Gy)	Nominal	**37.21** (19.44–59.93)	**37.34** (15.36 – 59.90)	**33.49** (11.91–58.34)
		Cumulative	**37.33** (14.26–60.33)	**38.01** (16.41–60.50)	**30.90** (9.26–59.88)
Oral cavity	D_{mean}(Gy)	Nominal	**15.27** (8.65–49.05)	**16.74** (11.37–54.70)	**11.09** (6.77–43.23)
		Cumulative	**15.90** (8.38–50.82)	**17.85** (11.08–56.55)	**12.15** (6.21–51.20)
Brainstem	D_{1cc}(Gy)	Nominal	**6.20** (0.55–17.14)	**5.45** (0.74–27.55)	**1.32** (0.34–16.26)
		Cumulative	**5.04** (0.47–17.11)	**4.97** (0.60–29.07)	**0.99** (0.43–15.08)
Healthy tissue	Integral dose (Gy*l)	Nominal	**59.79** (46.13–92.0)	**61.63** (49.67 – 96.74)	**49.82** (40.37–81.0)
		Cumulative	**61.43** (48.07–96.28)	**63.66** (53.40–101.13)	**51.76** (43.06–87.56)